

# NASA TECHNICAL MEMORANDUM

NASA TM X-64920

(NASA-TM-X-64920) GRAVITATIONAL CLOCK: A  
PROPOSED EXPERIMENT FOR THE MEASUREMENT OF  
THE GRAVITATIONAL CONSTANT G (NASA) 36 p HC  
\$3.75 CSCL 20J

N75-22974

Unclas

G3/46 19455

## GRAVITATIONAL CLOCK: A PROPOSED EXPERIMENT FOR THE MEASUREMENT OF THE GRAVITATIONAL CONSTANT G

By Larry L. Smalley  
Space Sciences Laboratory

January 24, 1975



**NASA**

*George C. Marshall Space Flight Center  
Marshall Space Flight Center, Alabama*

1. REPORT NO. NASA TM X-64920		2. GOVERNMENT ACCESSION NO.		3. RECIPIENT'S CATALOG NO.	
4. TITLE AND SUBTITLE Gravitational Clock: A Proposed Experiment for the Measurement of the Gravitational Constant G				5. REPORT DATE January 24, 1975	
				6. PERFORMING ORGANIZATION CODE	
7. AUTHOR(S) Larry L. Smalley*				8. PERFORMING ORGANIZATION REPORT #	
9. PERFORMING ORGANIZATION NAME AND ADDRESS  George C. Marshall Space Flight Center Marshall Space Flight Center, Alabama 35812				10. WORK UNIT NO.	
				11. CONTRACT OR GRANT NO.	
12. SPONSORING AGENCY NAME AND ADDRESS  National Aeronautics and Space Administration Washington, D.C. 20546				13. TYPE OF REPORT & PERIOD COVERED  Technical Memorandum	
				14. SPONSORING AGENCY CODE	
15. SUPPLEMENTARY NOTES      Prepared by Space Sciences Laboratory, Science and Engineering *Permanent Address: Dept. of Physics, University of Alabama in Huntsville, Huntsville, Alabama 35807. NAS/NRC Senior Postdoctoral Resident Research Associate.					
16. ABSTRACT  The increased importance and the fundamental significance of more accurately measuring the gravitational constant G are discussed herein. Recent or proposed experimental measurements of G are reviewed. The most promising method seems to be the use of mutually gravitating bodies in the "clock" mode in a drag-free satellite. In this view, a satellite experiment consisting of the flat-plate spherical mass oscillator proposed here combines the mathematical and experimental conveniences most simply. It is estimated that accuracies of 1 part in $10^6$ are easily obtainable simply by careful fabrication of parts. However, the use of cryogenic techniques, thin films, and superconductors should allow increased accuracies of two or three orders of magnitude or better. Hopefully, these measurements can be increased to the level of 1 part in $10^{11}$ at which time-variations, and other variations, in G can be observed.					
17. KEY WORDS			18. DISTRIBUTION STATEMENT  Unclassified-Unlimited  <i>Larry L. Smalley</i>		
19. SECURITY CLASSIF. (of this report)  Unclassified		20. SECURITY CLASSIF. (of this page)  Unclassified		21. NO. OF PAGES  37	22. PRICE  NTIS

# TABLE OF CONTENTS

	Page
I. INTRODUCTION .....	1
II. PRESENT STATE OF THE ART FOR OBSERVATIONS OF G ..	5
III. FLAT-PLATE SPHERICAL MASS OSCILLATOR .....	14
IV. CONCLUSIONS .....	26
REFERENCES .....	28

PRECEDING PAGE BLANK NOT FILMED

# LIST OF ILLUSTRATIONS

Figure	Title	Page
1.	Beams' balance configuration . . . . .	7
2.	An optically flat plate rotates below another flat plate that is suspended by a quartz-fiber . . . . .	7
3.	Two spheres of mass $M$ and radius $r$ mutually orbit each other at a radius $R \gtrsim 2r$ . . . . .	9
4.	A small test mass oscillates in a tunnel bored through a larger uniform density sphere . . . . .	9
5.	An earth-based version of the test mass oscillating in a tunnel of a larger sphere . . . . .	10
6.	A small cylindrical test mass is free to oscillate along the axis of a larger but hollow cylinder . . . . .	11
7.	In the double cruciform structure the rotor masses oscillate through tunnels bored in stator masses . . . . .	12
8.	The proof mass oscillates along an axis of a slot cut from a larger disc mass which itself rotates about an axis perpendicular to the orbital plane that is in the plane of the paper . . . . .	13
9.	Side view of a flat-plate, spherical mass oscillator . . . . .	15
10.	For a displacement of $\delta x$ of the small interior cylinder, the restoring force comes from a small slab of the outer cylinder of thickness $2\delta x$ a distance $L - \delta x$ away from the center of mass of the small cylinder . . . . .	16
11.	Geometry for calculating the gravitational potential between a thin hoop and a spherical mass on the axis of the hoop . . . . .	17

## LIST OF ILLUSTRATIONS (Concluded)

Figure	Title	Page
12.	Geometry for calculating the gravitational potential between a cylinder and a point mass on the axis of the cylinder . . . .	18
13.	Geometry for calculating the central force equation between two masses, $M_1$ and $M_2$ , in the presence of an earth of mass $M$ and with orbital angular velocity $\Omega$ . . . . .	22
14.	The masses oscillate perpendicular to the orbital plane as opposed to being in the plane as in Figure 13 . . . . .	24

## GRAVITATIONAL CLOCK: A PROPOSED EXPERIMENT FOR THE MEASUREMENT OF THE GRAVITATIONAL CONSTANT G

### I. INTRODUCTION

Historically, the gravitational constant, G, was the first fundamental constant measured. Yet, today, it is the least accurately known of all fundamental constants. This strange fact, until now, has been the result of two reinforcing circumstances: (1) the gravitational force is relatively very small, and (2) the gravitational constant is not necessary (important) in most practical physical problems; e. g., in electronics, or in planetary physics where G is not needed, and GM which can be measured astronomically very accurately is used. The irony of this situation is that since gravitational forces are small and purely mechanical, measurement of G is possible, in principle, to even greater accuracy than those constants that graze the domain of the quantum. Nevertheless, experimental obstacles have kept the accuracy of G to 1 part in  $10^3$ . However, through the use of space-age technology and satellite-borne experiments, most of these difficulties may be overcome, but this is not enough. All this would not be important except that the physical importance of knowing G very accurately has grown significantly in the last few years. The impetus for this knowledge is twofold: (1) the desire to test competing gravitational theories, and (2) experimental evidence of Van Flandern that G is changing with time [1].

Based on new and old observational data, Van Flandern concludes that from anomalous secular acceleration of the moon's mean longitude, the fractional rate change of G is

$$\frac{\dot{G}}{G} = -(8 \pm 5) \times 10^{-11}/\text{year} \quad . \quad (1)$$

Two alternate, but much less probable, explanations are a uniform expansion of all space or a solar system mass loss (presumably from the sun). The latter possibility is not consistent with actual solar mass losses, whereas a uniform expansion is ruled out (tentatively) since this implies a continuous increase in angular momentum; e.g., of the earth which is also not observed. Thus, the manifestly non-Einsteinian general relativistic result that  $\dot{G} \neq 0$  remains. However, it is a character of the Brans-Dicke-Jordan scalar-tensor theories that  $\dot{G}$  can be nonzero [2,3]. The same is true in the Vector-metric [4] or two-tensor metric theories [5] in which  $G$  is related to the second field. However, Van Flandern indicates [1] that his value of  $G$  [equation (1)] is more closely related to the cosmologies of Hoyle and Narlika [6] or that of Dirac [7] than with the Brans-Dicke theory. Van Flandern's contention about Brans-Dicke theories does not seem to be correct, since the value of  $G$  predicted by any scalar-tensor theory is strongly dependent on the value of poorly measured cosmological parameters such as the universe mass density and the deceleration parameter [8]. We must also contend with the possibility that there may be spatial variations in  $G$  such as occur, for example, in the scalar-tensor theories [9] or in Ni's new theory [10]. In general, this second type of variation of  $G$  can be summarized using the parameterized post-Newtonian (PPN) formalism [11] as indications of preferred frame effects or possible nonconservation of total four-momentum [9]. Preferred frame effects seem to be ruled out on the basis of experiment [9]. However, the experimental limits on some aspects of nonconservative theories in the PPN approximation have not been established, since these effects seem to be at or beyond our present experimental capabilities [9].

In the new PPN parameters, the spatial variation of  $G$  can be written as

$$G = 1 - (4\beta - \gamma - 3 - \zeta_2)U \quad , \quad (2)$$

where  $U$  is the gravitational potential,  $\beta$  and  $\gamma$  are the classical Robertson parameters (both equal to one in Einstein general relativity), and  $\zeta_2$  is one of four PPN parameters that indicates a possible nonconservative theory if non-zero [9]. In general,  $\zeta_2$  indicates a breakdown of the equivalence principle ( $M_{\text{passive}} \neq M_{\text{active}}$ ). [Possible preferred frame effects have been neglected in equation (2).] In the Brans-Dicke theory [9, 12],  $\beta = 1$ ,  $\gamma = (\omega + 1)/(\omega + 2)$ , where  $\omega$  is the usual Brans-Dicke coupling parameter and  $\zeta_2 = 0$  so that

$$(4\beta - \gamma - 3 - \zeta_2) = 1/(\omega + 2) \quad , \quad (3)$$

which then leads to spatial variations in  $G$ . However, these variations are still three or four orders of magnitude smaller than the best experimental accuracy of  $G$  [13, 14]. Recently Smalley<sup>1</sup> has shown that nonconservative theories, in particular theories for which  $T^{\mu\nu}_{;\nu} \neq 0$ , are possible; i.e., consistent with the field equations (Bianchi identities), gauge conditions on the metric, and the Newtonian limit of the conservation laws. One such theory, which is a modification of the Brans-Dicke theory, predicts the same PPN parameters with the exception that

$$\zeta_2 = \frac{8\sigma}{(2\omega + 3)^3}, \quad (4)$$

where  $\sigma$  is a coupling constant in the expression for the nonzero divergence of the energy-momentum tensor

$$T^{\mu}_{\nu;\mu} = \frac{\sigma}{8\pi} \phi^{;\mu} \phi_{;\mu} \phi_{;\nu} \quad (5)$$

and  $\phi$  is the scalar field. This theory agrees in all aspects, except for  $\zeta_2 \neq 0$ , with the usual Brans-Dicke theory. It should be contrasted with the original nonconservative scalar-tensor theory of Jordan [15] but does not, however, suffer from the criticisms of Fierz [16] or Bondi [17], at least at the level of PPN approximation. By comparing equations (3) and (4), it is possible that in a nonconservative Brans-Dicke theory the spatial variations in  $G$  could disappear; i.e., for the right choice of  $\sigma$ ,  $G = 1$  in equation (2). Thus, the violation of the strong principle of equivalence can be masked if the theory is also nonconservative, at least on the level of the PPN approximation. Thus we note that there are two competing effects which lead to variations in  $G$  — spatial and temporal variations — and, according to our discussion above, it is not certain whether a clear separation of the effects can be made.

Suppose we have a detector in orbit about the earth and we attempt to measure  $\dot{G}$ . Since the gravitational force is small, we know, a priori, that the experiment will be long term, perhaps lasting for months or a year. However,

---

1. Smalley, L. L.: Gravitational Theories with Nonzero Divergence of the Energy-Momentum-Tensor. To be published in The Physical Review.



the eccentricity of the earth's orbit about the sun will produce a 1 percent modulation of the solar gravitational potential  $U$  at the position of the earth, which could then produce a yearly spatial amplitude variation in  $G$  of<sup>2</sup>

$$\frac{\Delta G}{G} \approx 3 \times 10^{-11} \quad (6)$$

This variation is of the same order of magnitude as the temporal variation of  $G$  reported by Van Flandern. Therefore, any experiment that can determine  $G$  at the level of accuracy of 1 part in  $10^{11}$  must contend carefully with these competing effects. One possibility is a solar satellite with nearly zero eccentricity so that the temporal variations dominate or vice versa.

Finally, one last effect must be discussed. It has been tacitly assumed in this discussion that the Newtonian force law is an inverse square law. Although this may appear to be the same problem, it is not, but depends on the level at which general relativistic corrections become important. However, this test suffers identical experimental problems of accuracies of 1 part in  $10^4$  on the earth primarily because of errors in location of test masses [14, 18]. Until recently it was thought that the best test of the inverse square law came from the astronomical observations of the advance of the perihelion of Mercury. Long and Ogden have shown [19] that by using a double-ring source, very uniform gravitational fields can be produced in the laboratory. This means that if they consider the historic inverse-square-law failure in the form  $r^{-2 + \phi}$ , the advance of the perihelion of Mercury yields the limit,  $\phi < 4 \times 10^{-9}$ , whereas the use of their uniform laboratory fields could conceivably give a limit of  $\phi \approx 3 \times 10^{-12}$ . This stronger limit is, of course, directly related to the relatively lowered importance of positional accuracies for the test masses because of the highly uniform laboratory field.

Thus, it seems that an inverse-square-law failure could mask a spatial variation in  $G$ . Experimentally three intertwined effects remain that could conceivably introduce effects at the same order of magnitude. However, these three effects combine to enhance the theoretical importance of measuring  $G$  to higher accuracy if we hope to establish the correct gravitational theory. Most likely, these are questions we must answer before we can solve the important problems of initial data, quantum gravity, or unified field theory.

---

2. Weiss, R.: MIT internal report.

In Section II, recent attempts or proposed experiments for the determination of  $G$  are reviewed. However, recent work on null-experiments is omitted; i. e., Eötvös experiments that test the equivalence principle, except experiments that could conceivably be used to measure  $G$  directly. A satellite-borne gravitational clock experiment from which  $G$  can be obtained directly is proposed in Section III, and conclusions and some of the prospects for direct measurement of  $G$  are described in Section IV.

## II. PRESENT STATE OF THE ART FOR OBSERVATIONS OF $G$

It is one thing to say that  $G$  has been measured to 1 part in  $10^{10}$ , and it is entirely another to say that  $\dot{G}/G$  is known to the same value. The latter does not imply the former, not only because the value is model dependent, as in Van Flandern's work, but because a known variation in  $G$  never implies a knowledge of the magnitude of  $G$ . This becomes even more apparent when we recall that  $G$  is known at best to 1 part in  $10^4$  after several centuries of experimental and theoretical research [13].

Basically there are two ways to measure gravitational forces (following the outline of Weiss, previously cited in footnote 2): (1) by use of static mechanical or electrical forces such as springs, fibers, or electromagnetic devices; or (2) by gravitational inertia reaction forces. In the first category are the classical torsion balances of Cavendish and Eötvös and their modern improvements [20,21] as well as assorted electromechanical devices such as gravimeters, accelerometers, and gradiometers. The latter type of experiments can be generally classified as free-fall experiments, with the exception of the Beams' balance experiment [14,22] or the proposed rotating flat-plate experiment of Berman [23]. The primary difficulty with inertia experiments on the earth is suspension in the earth's gravitational field, which tends to overwhelm the dynamical effects.

Examples of free-fall inertia reaction experiments that have been proposed to measure  $G$  are:

1. Measuring the period of synchronously orbiting spheres by Berman and Forward [24] or Chapman (from the work previously cited in footnote 2).
2. Measuring the period of oscillation of a test mass through a bored hole in a larger spherical mass by Berman and Forward (from the work previously cited in footnote 2) and Berman [25], by a modification of the

proposed Worden and Everitt<sup>3</sup> Eötvös experiment, or by the flat-plate spherical mass oscillator proposed here.

3. Tangential acceleration balance by Blood (from the work previously cited in footnote 2), which is essentially a modification of the Beams' balance method. Weiss (see footnote 2) proposes to use the same experimental arrangement in a "clock" mode.

4. Centrifugal balance systems by Wilk (from the work previously cited in footnote 2), or through a modification of the rotating Eötvös force-balance proposed by Chapman [26,27].

We will touch, without mathematical details, on most of these experiments, stating briefly their methods, advantages, and disadvantages as well as their ultimate expectations.

As far as this author knows, there appear to be at present only two ongoing experiments to measure G: the ordinary, but supposedly improved sensitivity and experimentally isolated, torsion experiment of Cook and Marussi [20,21] and the constant angular acceleration experiment of Beams [14,22]. Also included here should be the active proposal of Worden and Everitt (see footnote 3) on which work on subsystem instrumentation is proceeding. However, this experiment is designed as an Eötvös experiment and would require modification along the lines of Weiss' modification, discussed below, of Blood's modified Beams' balance experiment (see footnote 2).

The standard torsion experiment (e.g., see Reference 18) seems to be limited by mechanical noise to accuracies somewhat less than 1 part in  $10^6$ , which Cook quotes as the limitation of their measurements of masses, lengths, and time. The Beams inertia reaction experiment (Fig. 1) features a rotating table accelerating with a constant angular acceleration. On the table are two large masses in a dumbbell arrangement which, when rotated about an axis perpendicular to their line of centers, produce a torque (T) on a small cylindrical bar. The experimental procedure is to compare the measured torque produced on the small cylinder with and without the large masses on the angularly accelerated table. The difference between these two torques allows one to calculate G directly. In their initial experiment, the small cylindrical mass was suspended by a quartz fiber, and ordinary bearings were used for the accelerating table [14,22]. Thus far, mechanical noise has limited the experiment to accuracies of about 1 part in  $10^4$ . The limiting accuracy seems

---

3. Worden, P. W.; and Everitt, C. W. F.: Test of the Equivalence of Gravitational and Inertial Mass Based on Cryogenic Techniques. Preprint, Stanford University, Jan. 1973.

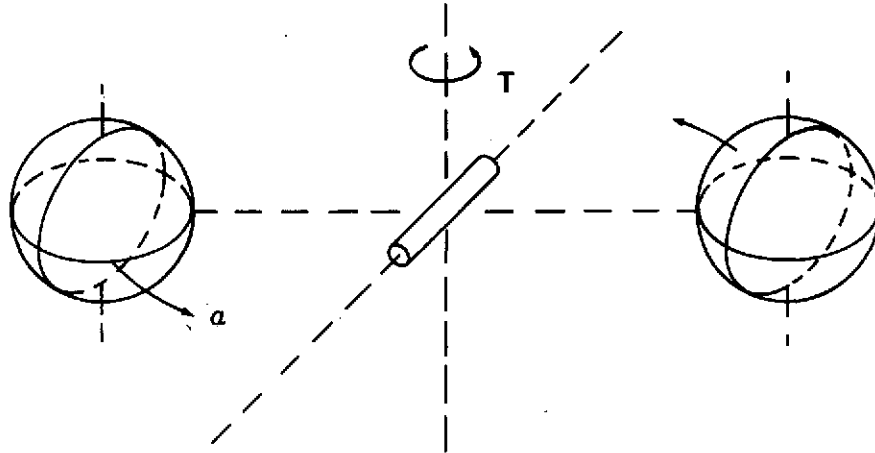


Figure 1. Beams' balance configuration (two large masses are constrained to accelerate with angular acceleration,  $\alpha$ , about a small cylinder; from the torque,  $T$ , sensed through the twisting of a quartz fiber about the vertical, the gravitational constant,  $G$ , can be calculated).

to be related to the certainty in the location of the center of mass of the two large spheres of about 5 parts in  $10^5$ . This then results in an ultimate design capability of 1 part in  $10^6$ , which they believe they can achieve providing they use magnetic suspension systems and/or air bearings.

A novel example of a proposed experiment for determining  $G$  is the rotating flat plate [23] depicted in Figure 2. In this experiment two optically flat and parallel rectangular solids are arranged so that one is suspended from a quartz fiber and is, therefore, free to oscillate with amplitude  $\theta$  about the vertical. The other plate is then driven with a uniform angular velocity about the same axis. The suspended plate then resonates

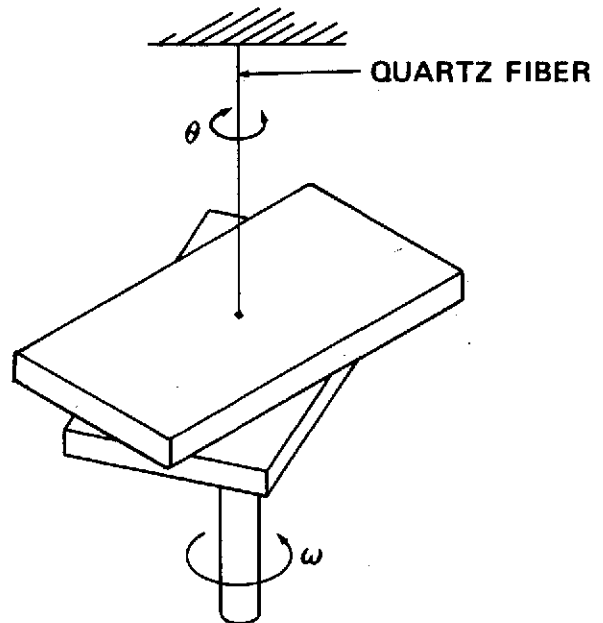


Figure 2. An optically flat plate rotates below another flat plate that is suspended by a quartz fiber (the gravitational constant can be obtained from the period of oscillation of the suspended plate about the vertical).

with some period from which  $G$  can be mathematically extracted providing anharmonics can be eliminated. By careful design, the fourth-order terms in  $\theta$  can be removed from the potential; but the forces (i. e., torques) are very small; and since the excitation mechanism depends on the second harmonic of the gravitational field, the sixth-order terms are important. Although physical dimensions can be fixed extremely accurately because of the nice optical properties of the plates, and since the system would be highly evacuated, it is purely a mechanical system and, therefore, mechanical noise limited. Thus, because the forces are so small, the accuracy of the system is limited by anharmonics and noise. Berman [23] estimates ultimate accuracies of about 1 part in  $10^5$ . Although not discussed by Berman, it is obvious that this experiment could operate in the constant angular acceleration mode similar to that of the Beams' balance. We have not as yet analyzed this possibility, but its simplicity is appealing.

In the first category of inertia reaction experiments are the miniature orbital systems such as, for example, that proposed by Berman and Forward [24] of two identical spherical masses,  $M$ , of radius  $r$ , in close orbit a distance  $R \gtrsim 2r$  apart as shown in Figure 3. A realistic period that depends on the density of the spheres and  $R$  is about 100 minutes. Although this system allows one to calculate  $G$  directly from the elementary centripetal equation

$$\Omega^2 = \frac{2GM}{R^3} \tag{7}$$

by measuring the orbital frequency,  $\Omega$ , the orbital radius,  $R$ , would be poorly determined and would be a major source of error limiting precision to about that of the older mechanical systems. Serious sources of error and limitation, not discussed for this particular experiment by Berman and Forward, are gravity and centrifugal gradients (with their own periods) that will tend to distort, nontrivially, the orbital motion of the spheres and their periods of rotation depending on the orientation of the orbital plane of the spheres with respect to the orbital plane of the satellite housing the experiment. We conclude, as they do, that this is not yet a practical laboratory experiment.

The second category of inertia experiments is the standard physics textbook problem, shown in Figure 4, of a test mass in free fall through a tunnel bored in a much larger sphere of uniform density. Such a free-fall system has also been investigated in detail by Berman and Forward [24], and there is even a modification by Berman [25], shown in Figure 5, that could be done on the surface of the earth by using a levered beam balance. However,

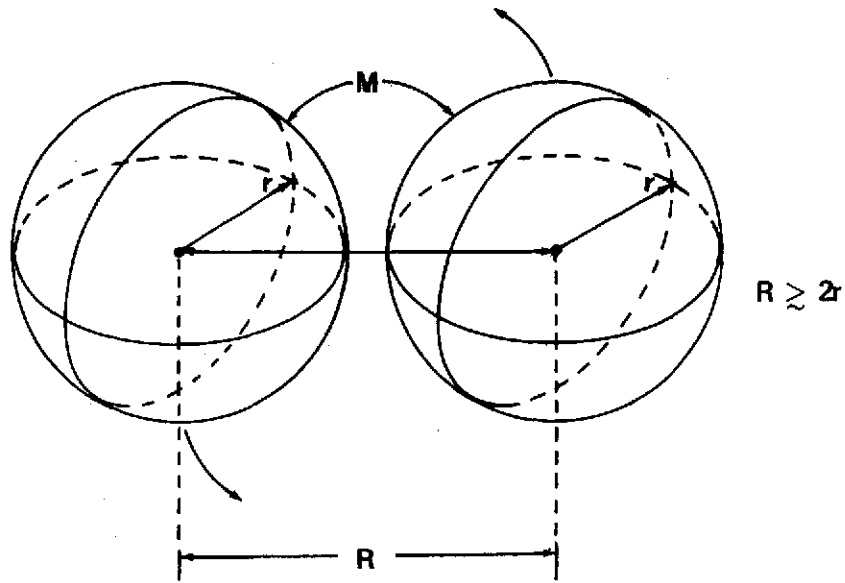


Figure 3. Two spheres of mass  $M$  and radius  $r$  mutually orbit each other at a radius  $R \geq 2r$ .

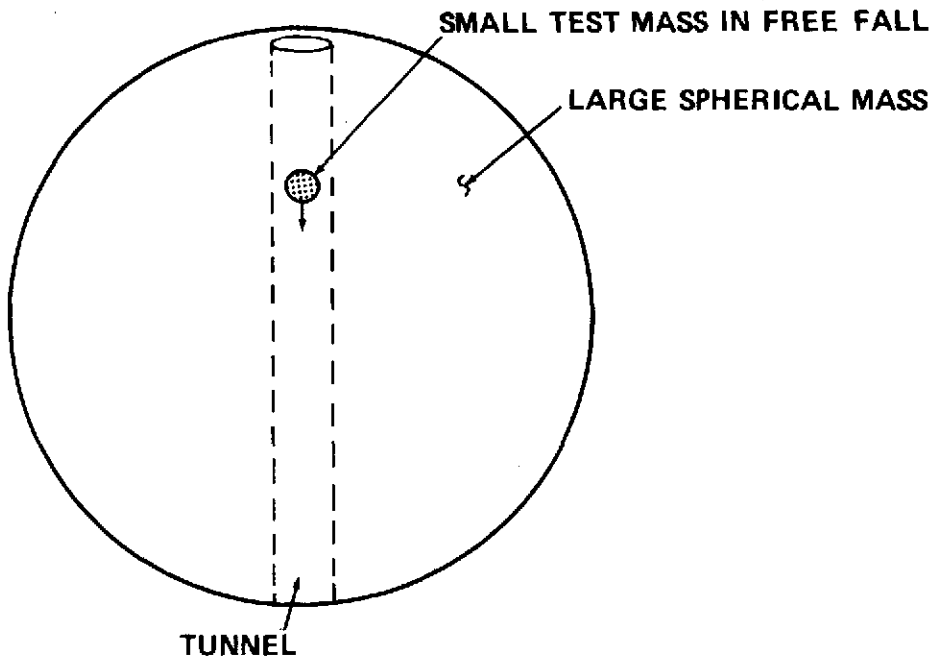


Figure 4. A small test mass oscillates in a tunnel bored through a larger uniform density sphere.

ORIGINAL PAGE IS  
OF POOR QUALITY

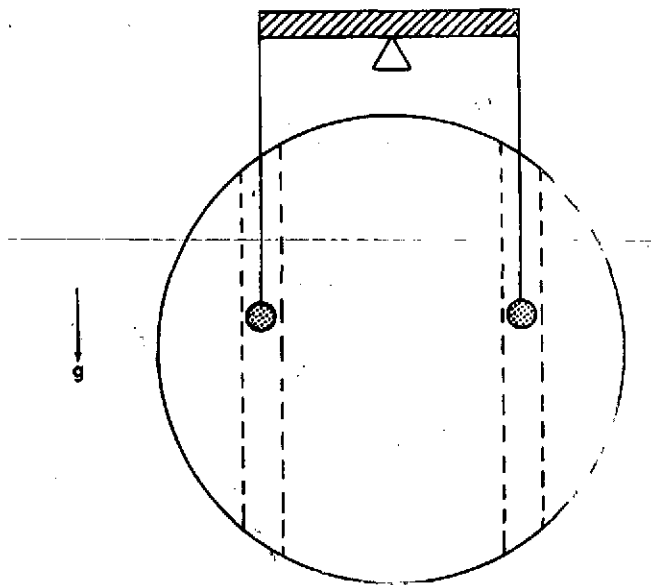


Figure 5. An earth-based version of the test mass oscillating in a tunnel of a larger sphere (the acceleration of gravity,  $g$ , is compensated for by a fulcrumed balance so that two small test masses can oscillate inside tunnels bored through the larger sphere).

gradients. The experimenters thus conclude that the only allowable orientation for the experiment is perpendicular to the orbital plane of the satellite along which axis the gradient forces are constant. Even so, the accuracy of the system is ultimately limited by determination of the radius and density variation of the larger sphere to about 1 part in  $10^6$ .

Worden and Everitt (see footnote 3) have proposed a free-fall Eötvös experiment in which a small cylinder is centered and parallel inside a larger cylinder, as shown in Figure 6. The acceleration which tends to decenter the masses would be a measure, among other possibilities, of a violation of the equivalence principle. Experimentally, no violation has been observed [28, 29] down to an Eötvös ratio of 1 part in  $10^{11}$ . However, their system, which is to be cryogenic and magnetically suspended and centered by superconducting coils, is theoretically capable of detecting an Eötvös ratio of 1 part in  $10^{19}$  but is experimentally limited at present by helium management to about 1 part in

Berman concludes that the earth-based experiment would not improve on the accuracy of  $G$  over the usual mechanical systems primarily because of gravity gradients and very serious alignment problems that would alter the period of oscillation significantly. However, the free-fall system of a test mass oscillating in a tunnel bored through a larger sphere bears more promise.

Again, this gives a direct measure of  $G$  from the period of oscillation of the test mass. However, because of nonspherical symmetry (after the tunnel is bored), the mathematics is no longer the simple theoretical problem originally proposed. In fact, the once obvious advantage of spherical symmetry is lost. Another limitation is the requirement for large amplitudes; otherwise there is no physical need in the first place for a tunnel through a large sphere. However, large amplitudes exacerbate gravity

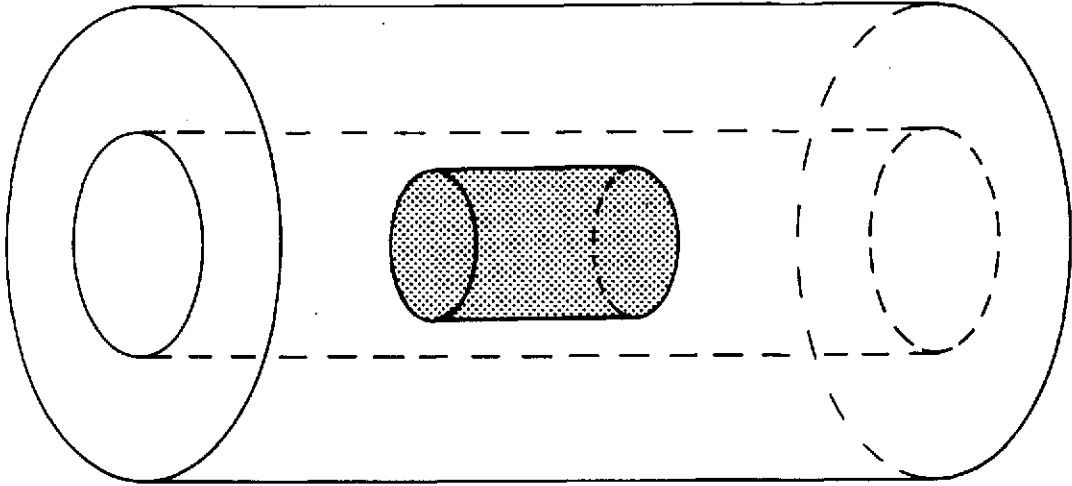


Figure 6. A small cylindrical test mass is free to oscillate along the axis of a larger but hollow cylinder.

$10^{14}$ , although they hope to improve this significantly in the near future by a better design of this subsystem. It is important to note that their system could be utilized in the oscillatory mode instead of using the acceleration signal in a feedback loop to a magnetic controller that continually centers the two masses. In fact, the controller system is a source of error since it introduces an oscillation about the null which then constitutes the minimum detectable reading. Fortunately, this error will be two or three orders of magnitude less than thermal noise. All other sources of error — such as gravity gradients, orbital eccentricity, differences in homogeneity of masses that cause a noncentering of the geometrical center with the center of mass (CM), non-coincidence of CM with the center of gravity (CG), asymmetrical satellite masses, residual drag-free satellite oscillations, magnetic forces, and residual gases —, they claim, can be detected and controlled so that thermal noise becomes the limiting source of error. However, an orbital eccentricity does not produce a driving harmonic oscillation of their system since such accelerations are proportional to amplitude in the same way that gradient forces are proportional to amplitude. Thus, looking at the Fourier component of the acceleration at orbital frequency as a source of error as in an Eötvös experiment will not work for the clock mode of operations. It is shown in the next section, in a discussion of the flat-plate spherical oscillator, that the system is essentially equivalent to a periodic Mathieu's equation instead of a driven harmonic oscillator. However, this is only a mathematical detail. Nevertheless, their experiment is well developed and has the immediate advantage of being able to perform two experiments, although the oscillator experiment has geometrical limitations which will be discussed later.



The third type of free-fall inertia experiment is a proposal by Weiss to modify Blood's tangential acceleration balance (see footnote 2) to a clock mode instead of uniformly accelerating one set of masses with respect to the other set (as in the Beams' balance). The tangential balance clock is basically a double cruciform structure (Fig. 7) with the central three masses, called the rotor, oscillating through tunnels bored in three larger exterior stator masses. Amplitude anharmonics can be reduced by design below the detection threshold for a proposed laser interferometer detection system capable of measuring fractional periods to  $10^{-8}$ . Although thermal noise is considered the fundamental limit to precision, Weiss claims that suspension problems limit the experiment to an ultimate measurement of G to 1 part in  $10^8$ .

The fourth and final category of inertia reaction experiments is the rotating Eötvös centrifugal force-balance system of Wilk (from the work previously cited in footnote 2) or Chapman [26, 27], which could also be

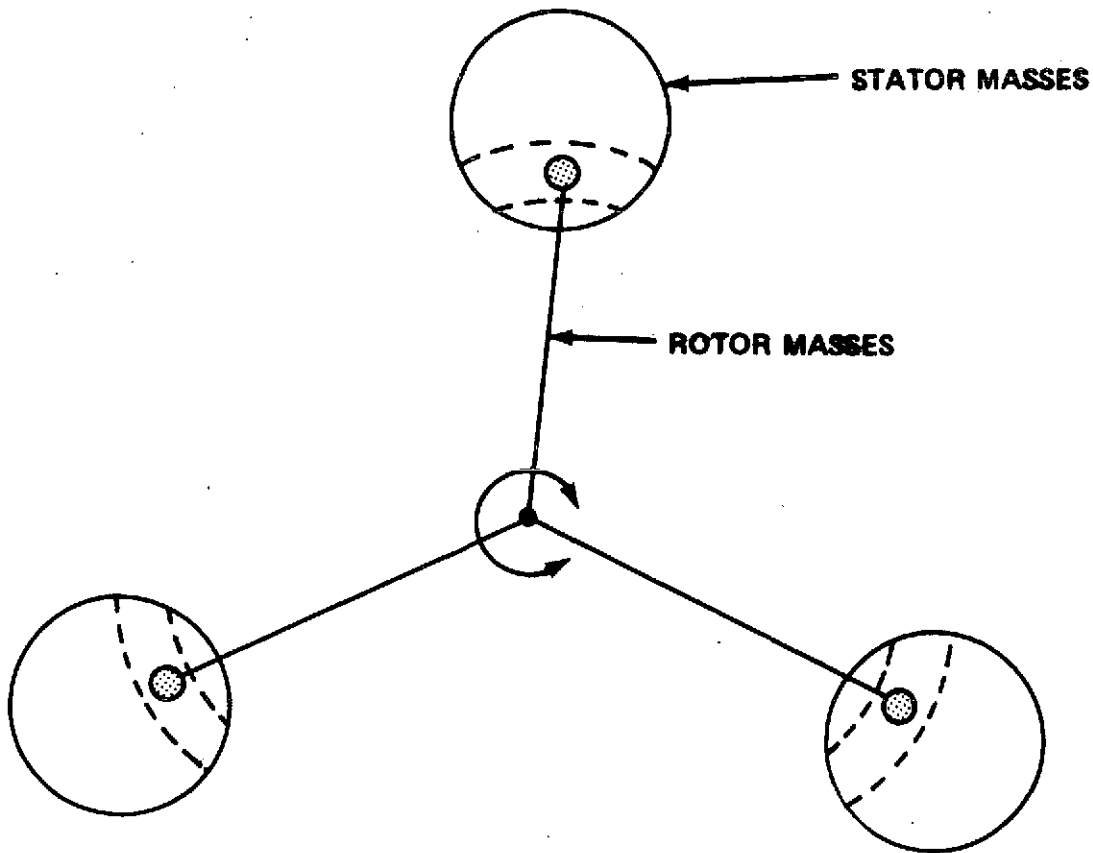


Figure 7. In the double cruciform structure the rotor masses oscillate through tunnels bored in stator masses.

operated in the clock mode for direct determination of  $G$ . In this type of satellite Eötvös experiment, a small proof mass is constrained to oscillate about the null position either mechanically or electromagnetically, as shown in Figure 8. In the clock mode this constraint is removed so that the small mass is free to oscillate along the accelerometer's sensitive axis under the mutual gravitational force between it and the larger mass. The right angular velocity of rotation of the larger disc mass and gravitational forces between the masses and cyclic gravity gradients then combine to restore the proof mass periodically toward the null position. The immediate advantage of this rotating system is that it attempts to compensate for gravity gradients through

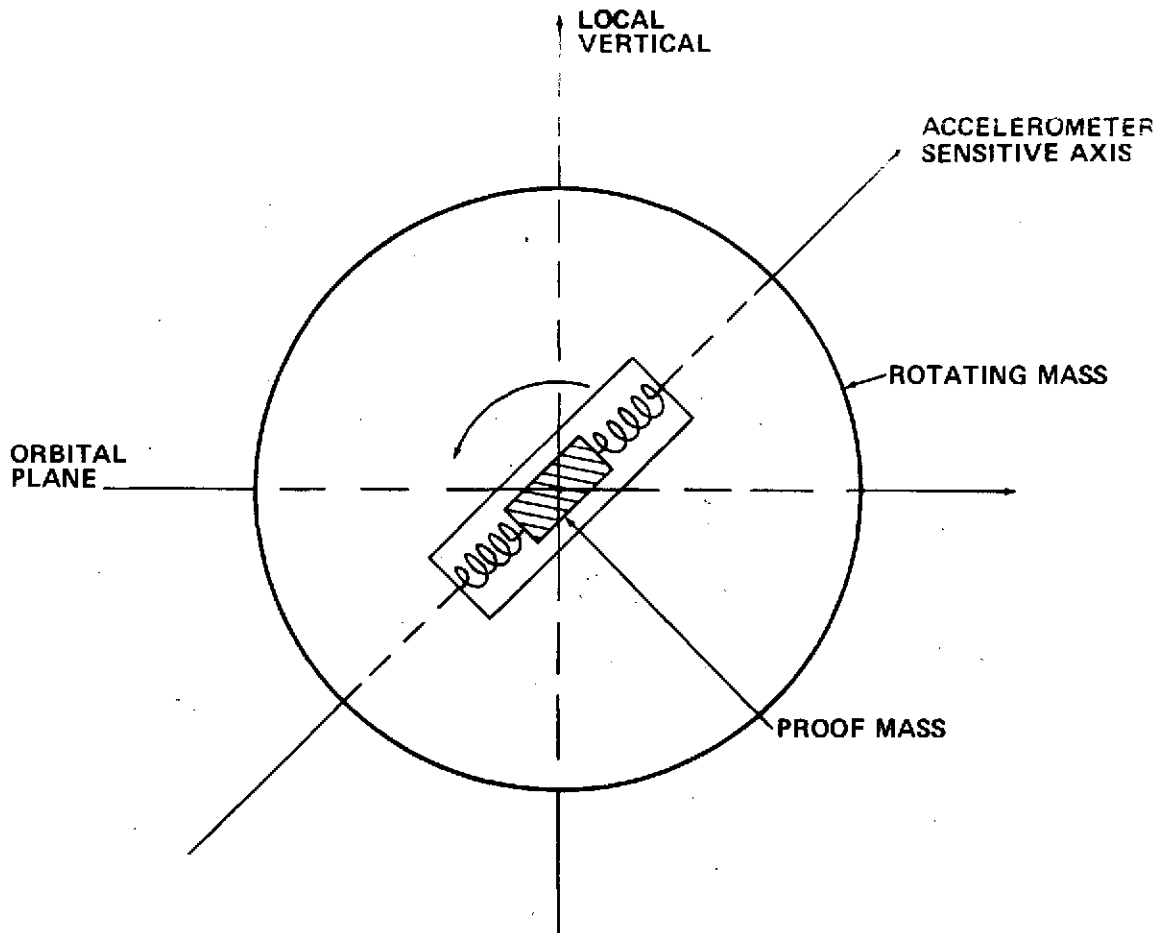


Figure 8. The proof mass oscillates along an axis of a slot cut from a larger disc mass which itself rotates about an axis perpendicular to the orbital plane that is in the plane of the paper.

centrifugal forces. The system is then described by a Mathieus' equation [30] of the form

$$\frac{d^2x}{dq^2} + (a - 2q \cos 2\xi)x = 0 \quad , \quad (8)$$

where  $a \lesssim 0$ , and  $q \gtrsim 0$  (see Section III). Unfortunately, its solution is only marginally stable since for small but negative  $a$  and  $q \gtrsim 0$ , it is near the border of the first instability region for the Mathieus' equation. If the system can be successfully operated in a stability region, the system is inherently as accurate as that of the double cylinder system of Worden and Everitt, provided cryogenic techniques and electromagnetic suspension are used. It should be understood that one does not neglect gravity gradient in the double cylinder experiment but that the system is easily operated in a stable mode, as will become obvious in the discussion of the flat-plate spherical mass oscillator in Section III. Another disadvantage of the rotating system is the method by which the system is rotated. This requires that the system be attached to a very stable, directionally oriented platform, whereas the cylindrical system or the flat-plate system is automatically stabilized along its own inertial axis and, thus, can fly "free" inside a larger "drag-free" satellite.

### III. FLAT-PLATE SPHERICAL MASS OSCILLATOR

Consider a cylindrically symmetric flat plate of radius  $c$  and height  $2\tau$  with a circular hole of radius  $b < c$  bored along an axis perpendicular to and centered on the flat ends of the cylinder. We then allow a spherically symmetric mass of radius  $b' \lesssim b$  to oscillate along this axis as shown in Figure 9. With the exception of the orbital mass systems, the combination of cylindrical and spherical symmetry is the simplest mathematical configuration that includes the effects of gravity and centrifugal gradients which can be used experimentally. Unfortunately, the more highly symmetric orbital system has severe experimental problems in determining the orbital radius, so that we are forced to consider a less symmetric system. Even the tunneled sphere problem depicted in Figure 4 is less symmetric because the tunnel destroys the useful spherical symmetry of the larger spherical mass. The cylindrical oscillator of Figure 6 has yet a lower symmetry, which implies a more untractable mathematical problem. However, these last two systems suffer experimental limitations that are somewhat circumvented by the inherent

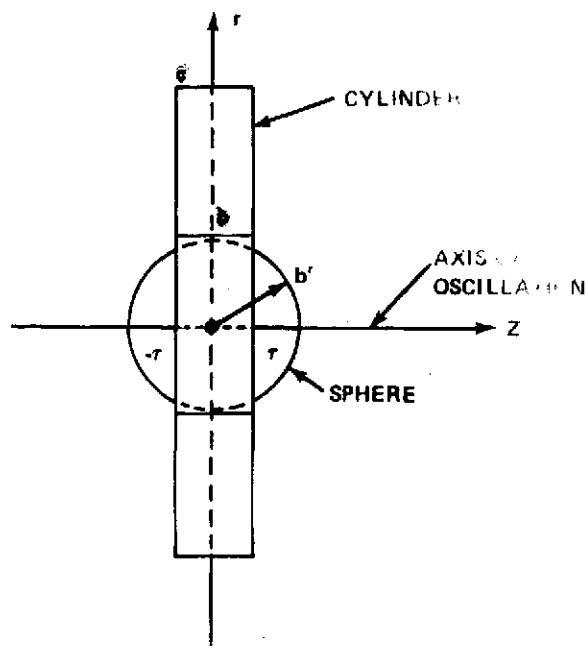


Figure 9. Side view of a flat-plate, spherical mass oscillator (the sphere of radius  $b'$  oscillates through a tunnel of radius  $b$  bored through a tunnel in the flat-plate cylinder of radius  $c$ ).

geometry of the orbital, flat-plate, spherical mass system. In the case of the totally cylindrical oscillator (Fig. 6), the gravitational restoring force tends to be smaller. This can be understood by noting that for a small displacement  $\delta x$  from the equilibrium position shown in Figure 10, the restoring force comes primarily from a slab of thickness  $2\delta x$  at the opposite end of the outer cylinder which then produces a relatively weaker restoring force. In the (ideal) large spherical system, the restoring force, as is well known, is due to the mass contained inside the mathematical sphere whose radius equals the test mass displacement from the center of the sphere along the tunnel. One, thus, has large excursions, which increases the relative importance of centrifugal and gravity gradients that increase with the radius and also are modulated by a time-dependent periodic function at

twice the orbital frequency for circular orbits. If the symmetry were exactly spherical, this would cause no problems, provided a stable mode is possible, since then the gravitational restoring force would also increase with radius. However, a tunnel of finite radius produces anharmonic amplitude effects which then require small amplitudes, and this implies a smaller attractive mass than for the flat-plate spherical mass oscillator. That is, for the flat-plate for an amplitude  $Z < 1$ , the attractive mass decreases as  $z$ , whereas for the sphere, it decreases as  $z^3$ . Thus, there appear to be both theoretical and experimental advantages for the flat-plate spherical mass oscillator over the other two oscillators described. However, this statement must be qualified to the point that the amplitude of oscillation remains small, but this results in another advantage.

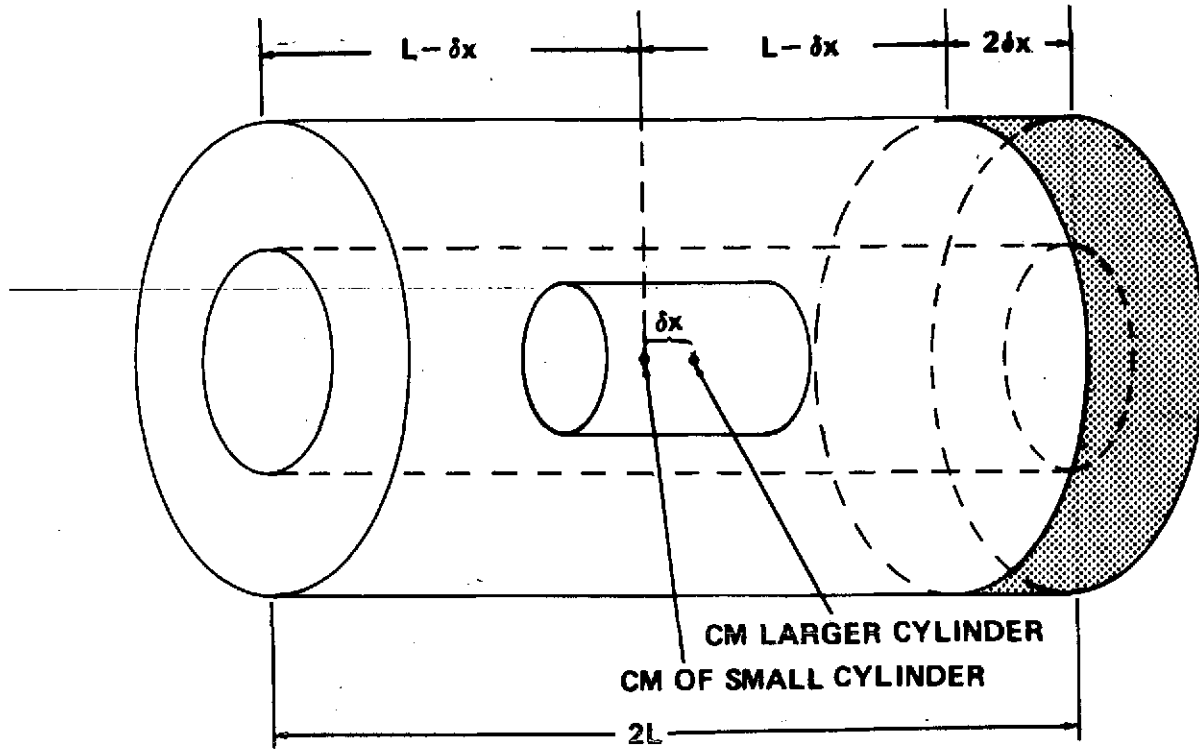


Figure 10. For a displacement of  $\delta x$  of the small interior cylinder, the restoring force comes from a small slab of the outer cylinder of thickness  $2\delta x$  a distance  $L - \delta x$  away from the center of mass of the small cylinder.

To demonstrate the mathematical simplicity of the flat-plate spherical mass oscillator, consider first Figure 11 which depicts a spherically symmetric mass of uniform density and radius  $r$  constrained to move along the axis of symmetry ( $z$  axis) of a thin hoop of radius  $\rho$  and surface density  $\lambda$ . The mass elements for the hoop are then

$$dM_h = \lambda \rho d\rho d\alpha \quad , \quad (9)$$

where  $\alpha$  is the angle of the differential of mass,  $dM_h$ , around the hoop, and the differential of mass for the sphere is given by

$$dM_s = \mu r^2 dr \sin \theta d\theta d\phi \quad , \quad (10)$$

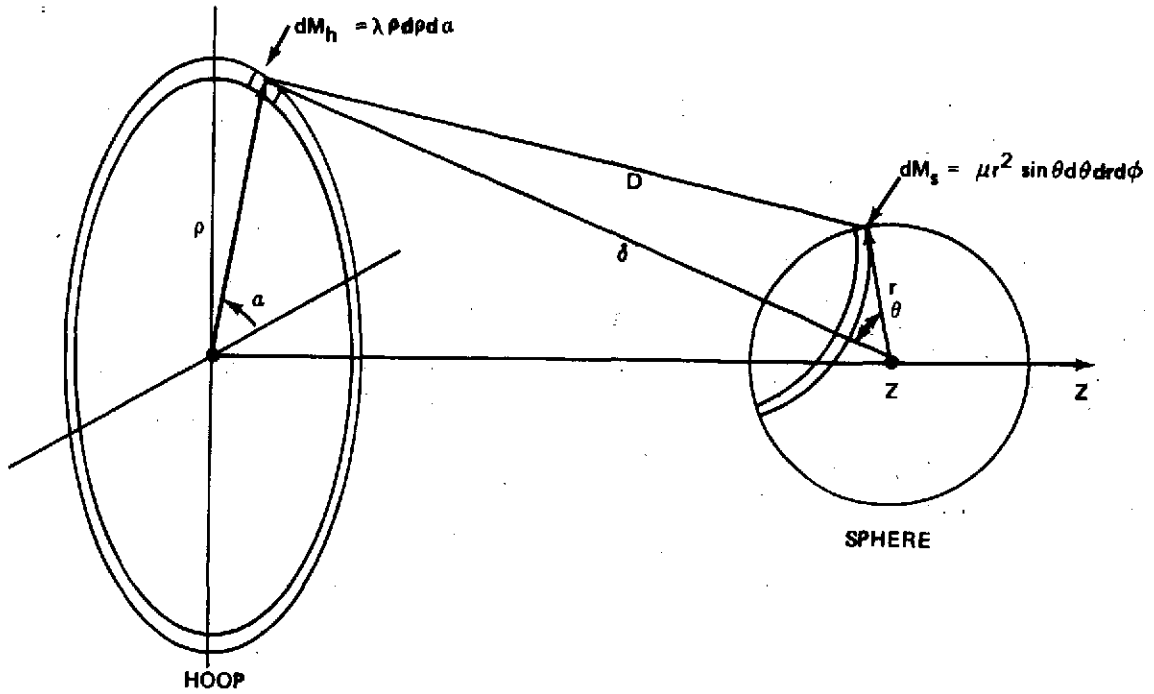


Figure 11. Geometry for calculating the gravitational potential between a thin hoop and a spherical mass on the axis of the hoop.

where  $\theta$  is the azimuthal angle measured from the line of length  $\delta$ , and  $\phi$  is the angle of rotation about this axis. We have then

$$\delta^2 = \rho^2 + z^2 \quad , \quad (11)$$

where  $z$  is the distance between the centers of mass and the distance  $D$  between mass elements is described by

$$D^2 = \delta^2 + r^2 - 2\delta r \cos \theta \quad . \quad (12)$$

The differential gravitational potential experienced by  $dM_h$  is then given by

$$d\phi = -dM_h G \int_{\text{sphere}} \frac{\mu r^2 \sin \theta d \theta d \phi dr}{D} = -\frac{GM_s dM_h}{\delta} \quad . \quad (13)$$

That is, we can treat the sphere as a point particle of mass  $M_s$  as long as the sphere is external to the hoop or to the generalization of the hoop into a short, hollow, right circular cylinder (Fig. 12) of height  $2\tau$ , centered at  $z = 0$ , and which has external radius  $c$  and internal radius  $b > b'$  where  $b'$  is the radius of the sphere. In this case, the potential at  $z$  becomes

$$\phi(z) = -GM_s \int_{\text{cyl}} \frac{2\pi\lambda\rho d\rho d\xi}{\delta} \quad , \quad (14)$$

where  $\lambda$  is now a uniform volume density and  $\xi$  is the variable of integration along the  $z$  direction and

$$\delta^2 = (z - \xi)^2 + \rho^2 \quad . \quad (15)$$

After the integration over  $\rho$ , we obtain

$$\phi(z) = 2\pi\lambda GM_s \int_{z+\tau}^{z-\tau} \left( \sqrt{c^2 + x^2} - \sqrt{b^2 + x^2} \right) dx \quad . \quad (16)$$

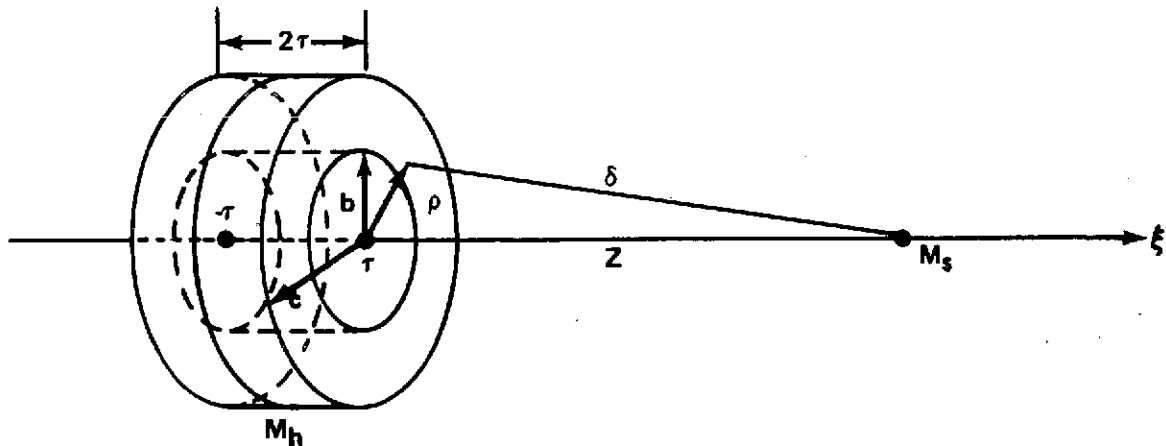


Figure 12. Geometry for calculating the gravitational potential between a cylinder and a point mass on the axis of the cylinder.

The force on  $M_s$  is then given by

$$\begin{aligned}
F_s(z) &= -\nabla\phi \Big|_z = -\frac{d\phi}{dz} \Big|_z \\
&= 2\pi\lambda GM_s \left[ \sqrt{c^2 + (z - \tau)^2} - \sqrt{b^2 + (z - \tau)^2} \right. \\
&\quad \left. - \sqrt{c^2 + (z + \tau)^2} + \sqrt{b^2 + (z + \tau)^2} \right] \\
&\approx 2\pi\lambda GM_s \tau \left\{ 2 \left( \frac{1}{\sqrt{b^2 + \tau^2}} - \frac{1}{\sqrt{c^2 + \tau^2}} \right) z \right. \\
&\quad \left. + \left[ \frac{c^2}{(c^2 + \tau^2)^{5/2}} - \frac{b^2}{(b^2 + \tau^2)^{5/2}} \right] z^3 \right\} , \quad (17)
\end{aligned}$$

where we have expanded for small  $z$ . To compare the effect of the  $z^3$  term, we consider the case where  $10^2\tau = 10b = c$  which yields the ratio of the third-order term to the second-order term,

$$\sim 5 \times 10^{-3} z^2 . \quad (18)$$

Thus, to reduce anharmonics (in this example) to an effect on the force of less than 1 part in  $10^{11}$ , we must keep amplitudes  $z \lesssim 10^{-4}$  cm. Although this amplitude is small, capacitive or magnetic-inductive tracking (see footnote 3) appears sensitive and accurate to  $0.05 \text{ \AA}$  so that small amplitude oscillations, we will find, permit a convenient mode of operation. Thus, we propose to operate the clock with the amplitudes that allow us to neglect the third-order term.

Define the quantity  $f_c$ , which is the ratio in equation (17) of the first-order term to  $z$ ,

$$f_c = 4\pi\lambda GM_s \tau \left( \frac{1}{\sqrt{b^2 + \tau^2}} - \frac{1}{\sqrt{c^2 + \tau^2}} \right) . \quad (19)$$



In terms of the mass of the plate

$$M_p = 2\pi\lambda\tau (c^2 - b^2) \quad (20)$$

then

$$f_c = \frac{2GM_p M_s}{(c^2 - b^2)} \left( \frac{1}{\sqrt{b^2 + \tau^2}} - \frac{1}{\sqrt{c^2 + \tau^2}} \right) \quad (21)$$

In the two-body central force problem, the frequency is related to the reduced mass  $\mu = M_p M_s / (M_p + M_s)$  so that

$$\omega^2 = \frac{f_c}{\mu} = \frac{2G(M_p + M_s)}{(c^2 - b^2)} \left( \frac{1}{\sqrt{b^2 + \tau^2}} - \frac{1}{\sqrt{c^2 + \tau^2}} \right) \quad (22)$$

For large  $c$  and  $\lambda = \rho = 16 \text{ g/cm}^3$ ,  $\omega^2 \approx 4\pi\rho G$ ; this implies a period of approximately 29 minutes.

Consider now the same oscillator in orbit with its axis of oscillation in the plane of the orbit. The total force on the two masses is due to three things: (1) the force due to each other, (2) the force due to the earth, and (3) gradient force due to centrifugal forces. This latter force, although a fictitious force, must be considered since we are in actuality dealing with an orbital problem for which the centripetal acceleration is given by

$$a_c = R\Omega^2 \quad (23)$$

where  $R$  is orbital radius and  $\Omega$  is orbital angular velocity. This implies that for small separation  $z_i$  from the center of mass, the  $i$ th particle of mass  $m_i$  will experience a repulsive centrifugal gradient force,

$$F_i = m_i z_i \Omega^2 \quad (24)$$

in the plane of the orbit. In the case of circular orbits

$$\Omega^2 = \frac{GM}{R^3} \quad , \quad (25)$$

where  $M$  is the mass of the earth. The total force on each part of the oscillator becomes

$$\left. \begin{aligned} M_1 \ddot{z}_1 &= f_c (z_2 - z_1) + \frac{GM_1 M}{R_1^2} \cos \alpha + M_1 z_1 \Omega^2 \\ M_2 \ddot{z}_2 &= f_c (z_1 - z_2) + \frac{GM_2 M}{R_2^2} \cos \beta + M_2 z_2 \Omega^2 \end{aligned} \right\} \quad , \quad (26)$$

where we have used the geometrical quantities defined in Figure 13, and the subscripts 1 and 2 refer, respectively, to the flat-plate and the spherical mass. In terms of the central force problem defined by the coordinate  $z = z_1 - z_2$  and the reduced mass  $\mu = M_1 M_2 / (M_1 + M_2)$ , we find that the central force problem can be described by the single equation

$$\mu \ddot{z} = -f_c z + G\mu M \left( \frac{\cos \alpha}{R_1^2} - \frac{\cos \beta}{R_2^2} \right) + \mu z \Omega^2 \quad . \quad (27)$$

Expanding  $R_1$  and  $R_2$  in terms of  $z_1/R$  and  $z_2/R$ , respectively, we obtain, after dropping higher order terms,

$$\begin{aligned} \mu \ddot{z} &= -f_c z + \frac{3G\mu M}{R^3} z \cos^2 \Omega t \\ &= - \left( f_c - \frac{3G\mu M}{2R^3} \right) z + \frac{3G\mu M}{2R^3} z \cos 2 \Omega t \quad . \end{aligned} \quad (28)$$

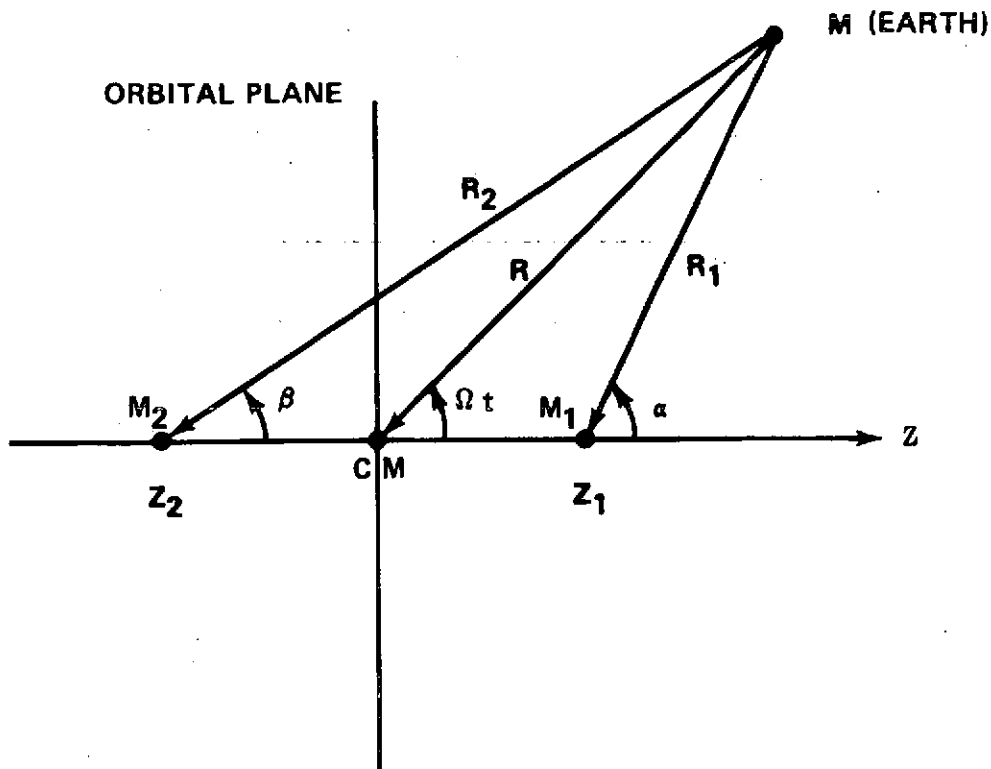


Figure 13. Geometry for calculating the central force equation between two masses,  $M_1$  and  $M_2$ , in the presence of an earth of mass  $M$  with orbital angular velocity  $\Omega$  (all three masses lie in the orbital plane).

Letting  $\Omega t = \xi$ , we then obtain the equation

$$\frac{d^2 z}{d\xi^2} + \left[ \left( \frac{f_c}{\mu \Omega^2} - \frac{3}{2} \right) - \frac{3}{2} \cos 2\xi \right] z = 0 \quad (29)$$

which can be compared with the general Mathieus' equation given in equation (8) with

$$\left. \begin{aligned} a &= \frac{f_c R^3}{GM\mu} - \frac{3}{2} = \frac{\omega^2}{\Omega^2} - \frac{3}{2} \\ q &= \frac{3}{4} \end{aligned} \right\} \quad (30)$$

Because the driving force in a Mathieus' oscillator is itself proportional to amplitude, it is not stable for arbitrary values of  $a$  and  $q$  as is the ordinary driven harmonic oscillator. For  $q = 3/4$ , stability requires that

$$-0.27 \leq a \leq 0.18 \quad (31)$$

for the first region of stability. The second region of stability begins at about  $a \geq 1.72$  which represents an upper bound (as if the boundary could be represented by a straight line). From equation (30), we find

$$1.23 \leq \frac{\omega^2}{\Omega^2} \leq 1.68 \quad ,$$

$$\frac{\omega^2}{\Omega^2} \geq 3.22 \quad , \quad (32)$$

and so forth. For a given set of masses (and geometry), the stability regions depend on the orbital radius through  $\Omega$ ; these regions then oscillate with altitude. We now note the unusual consequence of the Mathieus' equation: stable operation requires that the oscillator frequency be greater than the orbital frequency; i. e., the character of the solution is very much different from that of a driven harmonic oscillator. However, within the stable ranges, it is possible to extract  $G$  from knowledge of both the period and the amplitude of oscillation.

Another mode of operation occurs when the oscillator axis is perpendicular to the orbital plane as depicted in Figure 14. In this case

$$\ddot{z} + \left( \frac{f}{\mu} + \frac{GM}{R^3} \right) z = 0 \quad (33)$$

is an ordinary harmonic oscillator with frequency  $\omega_{\perp}$  given by

$$\omega_{\perp}^2 = \frac{f}{\mu} + \frac{GM}{R^3} = \omega^2 + \Omega^2 \quad . \quad (34)$$

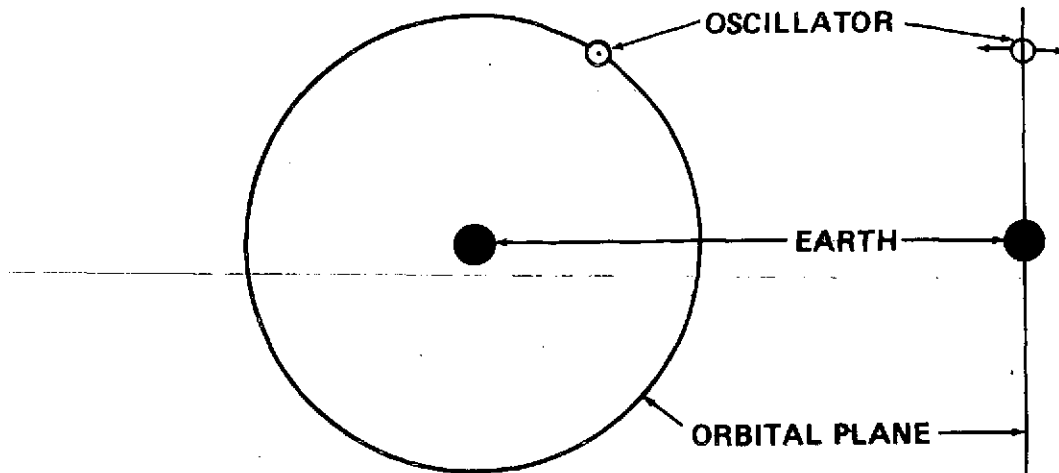


Figure 14. The masses oscillate perpendicular to the orbital plane as opposed to being in the plane as in Figure 13.

Since the quantity  $\Omega$  can be accurately determined from orbital tracking data,  $G$  can be easily extracted from equation (34) after measuring  $\omega_{\perp}$ . On the other hand, if the experiment is operated at several different altitudes, knowledge of  $\omega_{\perp}(R)$  allows one to extract both  $G$  and  $M$  from the data.

Thus, if we include this mode of operation along with that of the oscillator axis in the orbital plane, there are three independent ways to extract  $G$  from the data.

It should be pointed out that the above calculations assume perfectly circular orbits. Noncircular orbits introduce orbital frequency harmonic and subharmonic terms into the force described by equation (28). The largest perturbation is at orbital frequency instead of the twice orbital effect given in equation (28) but is proportional to the orbital eccentricity,  $\epsilon$ . Thus, for circular orbits with  $\epsilon < 10^{-6}$ , we can neglect these effects on frequency and amplitude measurements for the oscillator.

Because of geometrical considerations, the radius of the sphere will not be known as accurately as the dimension of the flat plate, which can be fabricated more accurately. However, the uncertainty in the radius of the sphere (i.e., the mass of the sphere) because of spherical symmetry can be transferred into an uncertainty in  $z$ . For a small uncertainty of about 1 part in  $10^6$ , which seems feasible, this contribution to the period is negligible. In principle, the period is simply related to the total masses and the overall geometry. Nonuniform density does, however, produce an uncertainty in the

position of the CM of the sphere and flat plate which tends to produce a torque because of the nonuniformity of the gravitational potential of the flat plate over the volume of the sphere. This torque then produces a periodic rotation of the sphere with respect to the plate which is a direct determination of the inhomogeneity of the sphere. Very accurate determination of these rotations is possible through the detection of the London moment produced by a rotating superconductor.

To monitor the oscillations of the sphere, we propose to enclose the spherical mass inside a thin spherical shell rigidly attached to the flat plate. Because of the spherical symmetry of the shell, the shell does not affect the motion of the spherical mass. The oscillator will then be constrained to move along one dimension by using a capacitance controller attached to the shell that can also record the amplitude and frequency of oscillations along the active axis. Superconducting loops can also then be attached to the shell, and by use of Josephson bridges, the rotation of the sphere can be measured.

The measuring system introduces so-called tracking errors which, for instance, in an Eötvös null system would produce a feedback oscillation that would then represent the minimum detectable motion of the system. Worden and Everitt (see footnote 3) have discussed this type of error and conclude that it is much less than amplitudes expected from thermal noise which can be approximated by

$$\langle \Delta x \rangle \sim \sqrt{\frac{kT}{\mu\omega^2}} \quad , \quad (35)$$

where  $k$  is the Boltzmann constant and  $T$  is temperature. For a period of 1 hour,  $\mu = 10$  kg,  $T = 3k$ , then  $\langle \Delta x \rangle \sim 10^{-7}$  cm. The minuteness of the thermal errors compared with a signal of  $10^{-4}$  cm is, of course, partially due to the fact that the clock is a dynamical experiment and that both components of the clock are relatively large compared with, for example, the small rod in Beams' experiment; i. e., small components are not necessary.

Another potential source of error is due to the mode of operation — free active axis for the clock as opposed to null centering in the Eötvös experiment. As a result, the capacitance controller will tend to produce cross-talk between the passive axes and the active axis of the system when the sphere moves off the equilibrium position along the active axis. These forces arise when the sphere moves out of its equilibrium position and hence its symmetry position

with respect to the capacitors, thus giving rise to a restoring force. However, this type of force, although much larger than the gravitational force, can be compensated for electronically at the same level of measurement accuracy of the controller itself and, therefore, will not affect the gravitational restoring force and its clock mode of operation.

The main source of error in the experiment comes not from the determination of the period of oscillation but from the accurate determination of  $f_c$  given in equation (21). If we assume the conservative estimates of others, all quantities such as mass, density, and dimension can be obtained to accuracies of about 1 part in  $10^6$ .

#### IV. CONCLUSIONS

The flat-plate spherical mass oscillator was considered as a method for obtaining  $G$  for the following reasons:

1. It is mathematically the simplest system.
2. Internal gravitational forces were relatively large.
3. The control and measurement systems are relatively simple because one member of the oscillator is spherical.

To this list we could add that the dimensions of the flat plate can also be fabricated more accurately than for spheres. Thus, for a given accuracy of measuring lengths, one has an inherently more accurate determination of  $G$ . The effects of density variations can be measured and be ultimately compensated for in calculations of  $G$ .

Since the experiment is relatively simple, the experiment can be duplicated with different substances (change  $\rho$ ), and different masses (change  $c$ ,  $b$ ,  $b'$ ,  $\tau$ ). One then obtains parametric curves  $\omega^2(G, \rho, c, b, b', \tau)$  from which  $G$  can be extracted with a higher degree of confidence than from any individual experiment.

When one has confidence in a more accurately known  $G$ , one can perform Kreuzer-type experiments [31] that can experimentally determine the equivalence of active and passive gravitational mass by simply constructing the two parts of the oscillator out of different substances. (Compare this with the Eötvös experiment that compares inertial versus gravitational mass.)

Finally, even without using experimental techniques comparable to those necessary in the satellite superconducting gyroscope experiment or that proposed in the Eötvös experiment of Worden and Everitt, accuracies of 1 part in  $10^6$  would easily be obtained without concern for more than fabrication accuracies and measurement of the period of oscillation. However, measuring density fluctuations and correcting for their effects on the periods of oscillations, taking the orbital eccentricity into account, using large components, low temperature, and superconductivity, and integrating observations over long periods by use of stable atomic clocks would increase the accuracy conservatively by at least two or three orders of magnitude.

At the level of accuracy of 1 part in  $10^8$  or better, it then becomes important to consider spatial variations in  $G$  or failures in inverse square law. To disentangle these effects may require the use of orbits of high eccentricity, solar satellites, or both. At any rate, a second independent experimental determination of variations of  $G$ , presumably by accurately determining the magnitude of  $G$  as a function of both space and time, is of fundamental importance to science.



## REFERENCES

1. Van Flandern, T. C.: *Mon. Not. Roy. Astr. Soc. (London)*, vol. 170, 1975, p. 333.
2. Jordan, P.: *Z. Phys.*, vol. 157, 1959, p. 112.
3. Brans, C.; and Dicke, R. H.: *Phys. Rev.*, vol. 124, 1961, p. 925.
4. Hellings, R. W.; and Nordtvedt, K., Jr.: *Phys. Rev.*, vol. D7, 1973, p. 3593.
5. Lightman, A. P.; and Lee, D. L.: *Phys. Rev.*, vol. D8, 1973, p. 3293.
6. Hoyle, F.; and Narlika, J. V.: *Mon. Not. R. Astro. Soc.*, vol. 155, 1972, p. 323.
7. Dirac, P. A. M.: *Proc. R. Soc. Lond.*, vol. A333, 1973, p. 403.
8. Weinberg, S.: *Gravitation and Cosmology: Principles and Applications of the General Theory of Relativity*. Wiley, New York, 1972, pp. 619-631.
9. Will, C. M.; and Nordtvedt, K.: *Ap. J.*, vol. 177, 1972, pp. 757, 775.
10. Ni, W. T.: *Phys. Rev.*, vol. D7, 1973, p. 2880.
11. Will, C. M.: *Ap. J.*, vol. 163, 1971, p. 611.
12. Nutku, Y.: *Ap. J.*, vol. 155, 1969, p. 999.
13. Recommended Unit Prefixes; Defined Values and Conversion Factors; General Physical Constants. National Bureau of Standards Miscellaneous Publication No. 253, U.S. Government Printing Office, Washington, D.C., 1963.
14. Rose, R. D.; et al.: *Phys. Rev. Letters*, vol. 23, 1969, p. 655.
15. Jordan, P.: *Nature*, vol. 164, 1949, p. 637.

## REFERENCES (Continued)

16. Fierz, M.: *Helv. Phys. Acta.*, vol. 29, 1956, p. 128.
17. Bondi, H.: *Cosmology*. Cambridge University Press, 2nd edition, 1960, p. 163.
18. Heyl, P.; and Chryanowski, P.: *J. Res. Nat. Bur. Stand.*, vol. 29, 1942, p. 1.
19. Long, D. R.; and Ogden, D.: *Phys. Rev.*, vol. D10, 1974, p. 1677.
20. Cook, A. H.: "The Experimental Determination of the Constant of Gravitation," as reported in *NBS Precision Measurements and Fundamental Constants*. Available from National Technical Information Service, Springfield, Virginia, 1972, pp. 475-483.
21. Cook, A. H.: *Contemp. Phys.*, vol. 9, 1968, p. 227.
22. Towler, W. R.; Parker, H. M.; Lowery, R. A.; Kuhlthau, A. R.; and Beams, J. W.: "Measurement of Newtonian Gravitational Constant G," as reported in *NBS Precision Measurements and Fundamental Constants*. Available from National Technical Information Service, Springfield, Virginia, 1972, pp. 485-492.
23. Berman, D.: "Discussion and Analysis of the Rotating Flat Plate Newtonian Gravitational Constant Experiment," as reported in *Research Toward Feasibility of an Experiment for Measuring Vertical Gradients of Gravity, Appendix F, Final Report, Air Force Contract AF19(628)6134*.
24. Berman, D.; and Forward, R. L.: *Free-Fall Experiments to Determine the Newtonian Gravitational Constant (G)*. Paper presented to American Astronautical Society, 14th Annual Meeting, Dedham, Mass., May 13-15, 1968.
25. Berman, D.: "Discussion and Analysis of the Vertically Tunneled Sphere — Newtonian Gravitational Constant Experiment," as reported in *Research Toward Feasibility of an Experiment for Measuring Vertical Gradients of Gravity, Appendix G, Final Report, Air Force Contract AF19(628)6134*.

## REFERENCES (Concluded)

26. Chapman, P. K.: "Gravitational Experiments in Manned Spaceflight," as reported in Space Systems and Thermal Technology for the 70's. Part I, Proceedings, American Society of Mechanical Engineers Space Technology and Heat Transfer Conference, Los Angeles, Calif., June 21-24, 1970.
27. Chapman, P. K.; and Hanson, A. J.: Proceedings of the Conference on Experimental Tests of Gravitational Theories. Jet Propulsion Laboratory TM33-499, Nov. 1970, pp. 228-235.
28. Roll, P. G.; Krothkov, R.; and Dicke, R. H.: Annals of Phys., vol. 26, 1964, p. 442.
29. Braginskii, V. B.; and Panov, V. I.: Soviet Phys. JETP, vol. 34, 1971, p. 464.
30. Blanch, G.: "Mathieu Functions," in Handbook of Mathematical Functions. Ed. by M. Abramowitz and I. A. Stegun, AMS55, National Bureau of Standards, U.S. Government Printing Office, 1965, pp. 721-750.
31. Kreuzer, L. B.: Phys. Rev., vol. 169, 1968, p. 1007.


# APPROVAL

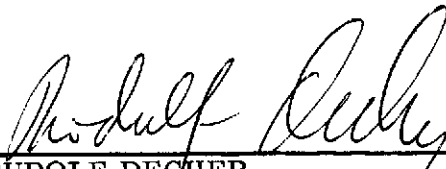
## GRAVITATIONAL CLOCK: A PROPOSED EXPERIMENT FOR THE MEASUREMENT OF THE GRAVITATIONAL CONSTANT G


By Larry L. Smalley

The information in this report has been reviewed for security classification. Review of any information concerning Department of Defense or Atomic Energy Commission programs has been made by the MSFC Security Classification Officer. This report, in its entirety, has been determined to be unclassified.

This document has also been reviewed and approved for technical accuracy.

  
\_\_\_\_\_  
EUGENE W. URBAN  
Chief, Low Temperature and Gravitation  
Sciences Branch

  
\_\_\_\_\_  
RUDOLF DECHER  
Chief, Radiation and Low Temperature  
Sciences Division

  
\_\_\_\_\_  
CHARLES A. LUNDQUIST  
Director, Space Sciences Laboratory

# DISTRIBUTION

## INTERNAL

ES01

C. Lundquist  
A. Tingle (2)

ES11

W. Snoddy

ES21

R. Decher

ES24

E. Urban  
L. Holdeman  
P. Eby  
L. Smalley (25)

ES31

R. Naumann

ES41

W. Vaughan

AS61 (2)

AS61-L (8)

AT01 (6)

CC

Mr. Wofford

## EXTERNAL

Dr. John Hendricks

Physics Department

The University of Alabama in Huntsville

P.O. Box 1247

Huntsville, AL 35807

Dr. Jerry Karr

Physics Department

The University of Alabama in Huntsville

P.O. Box 1247

Huntsville, AL 35807

Dr. Francis Everitt

W. W. Hanson Lab. of Physics

Stanford University

Stanford, CA 94305

Scientific and Technical Information  
Facility (25)

P.O. Box 33

College Park, MD 20740

Attn: NASA Representative (S-AK/RKT)

Dr. J. E. Rush

Dean Graduate Study and Research

The University of Alabama in Huntsville

Huntsville, AL 35807

Dr. J. Hoomani

Dean Science and Engineering

The University of Alabama in Huntsville

Huntsville, AL 35807

Dr. Rainer Weiss

Room 20F001

Massachusetts Institute of Technology

Cambridge, MA 02139